

GPS-DENIED NAVIGATION USING SAR IMAGES AND NEURAL NETWORKS

Teresa White¹, Jesse Wheeler², Colton Lindstrom³, Randall Christensen³, Kevin R. Moon¹

¹Dept. Mathematics & Statistics, ³Dept. Electrical & Computer Engineering—Utah State University
²Dept. Statistics—University of Michigan



4
0
6
2

Introduction

Precise navigation data is necessary for autonomous vehicles.

- In normal circumstances: GPS is typically used

PROBLEM:

Error	Shift Direction	Blur Direction
AT Position	AT	None
CT Position	CT	None
D Position	CT	None
AT Velocity	None	AT
CT Velocity	AT	None
D Velocity	AT	None
AT Attitude	None	Small AT
CT Attitude	None	Small AT
D Attitude	None	Small AT

- GPS may not always be available
- We use synthetic aperture radar (SAR) images to estimate the navigation data.
- The Back-projection Algorithm (BPA) is used to create SAR images [1].
- Any error in position, velocity, or attitude results in distorted SAR images [2].
- Different navigation error combinations create subtly different image distortions.

Table 1: Effect of navigation errors on BPA-SAR images (AT = Along Track; CT = Cross Track; D = Down).

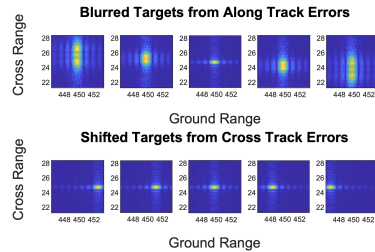


Fig. 1: Blur (Top) and shift (Bottom) distortions caused by navigation errors in AT velocity and CT position, respectively.

- Any error in position, velocity, or attitude results in distorted SAR images [2].
- Different navigation error combinations create subtly different image distortions.

SOLUTION:

- We use convolutional neural networks (CNN) to estimate initial navigation errors from distorted SAR images.
- True flight trajectory is recovered from the initial navigational errors [2].
- We compare distorted images to previously-obtained reference images.

The SAR Data

Three different sets of SAR image data:

- Simulated data: 5 second aperture length (MATLAB)
- Real datasets: 2 and a 10 second aperture lengths (Space Dynamics Laboratory)

Scenario #	AT Pos	CT Pos	D Pos	AT Vel	CT Vel	D Vel
1	X	X				
2				X	X	
3	X	X	X	X	X	
4	X	X	X			
5				X	X	X
6	X	X	X	X	X	X

Table 2: Summary of scenarios and corresponding initial errors. Each "x" on the table indicates whether the error state was considered.

For each of the datasets, six different scenarios were studied.

Dataset	Training		Validation		Testing	
	# targets	# images	# targets	# images	# targets	# images
Sim-5-sec	134	13500	19	1900	39	3800
Real-2-sec	130	13000	18	1800	37	3700
Real-10-sec	122	12300	17	1700	36	3500

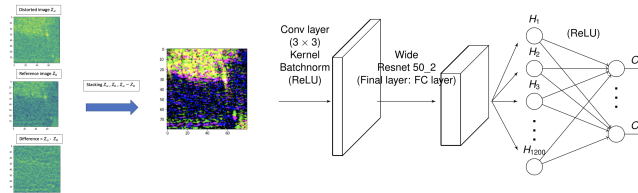
Table 3: Training (70%), validation (10%), test (20%) set.

- For each target, we generated 100 distorted images of size 80 × 80 pixels, paired with the corresponding navigation errors.

- Navigational errors are standardized to ensure equal consideration during training.

Neural Network Architecture

- We used transfer learning with the pretrained Wide ResNet 50_2 architecture forming the base of our model [3].
- Our model:
 - Input: the distorted image, reference image, and the difference image.
 - Input is fed into a randomly initialized convolutional layer followed by the ResNet architecture.
 - ResNet final layer replaced with a fully connected layer with same output number as error states.



- L2 regularization and the average mean squared error (MSE) loss function was used across all considered initial errors for training and testing:

$$MSE = \frac{1}{mn} \sum_{\alpha=1}^n \sum_{\beta=1}^m (s_{\alpha\beta} - \hat{s}_{\alpha\beta})^2,$$

[m] : Number of error states considered

[n] : Number of training images in the data

[s_{αβ}] : True standardized error of the βth error and the αth image

[ŝ_{αβ}] : Corresponding error estimate by the neural network

- MSE less than one indicates that the neural network is learning relevant information for this task.

Experimental Results

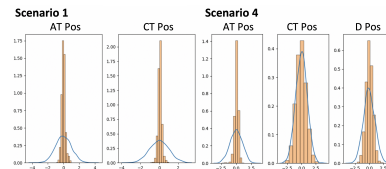


Fig. 2: Distribution of Error States before (blue line) and after (histogram) estimation for real-2-sec dataset for scenarios 1 and 4.

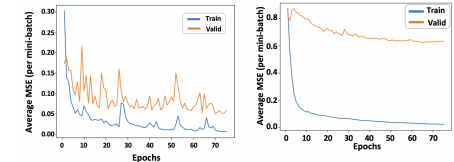


Fig. 3: Training and validation MSE as a function of training epoch for scenario 1 (Left) and for scenario 2 (Right) for the real-2-sec dataset. A large gap between the training and validation error suggests the network may be overfitting.

Scenario #	Dataset	AT Pos	CT Pos	D Pos	AT Vel	CT Vel	D Vel
1	MSE (Sim-5-sec)	0.0594	0.0289	N/A	N/A	N/A	N/A
	MSE (Real-2-sec)	0.0563	0.0425	N/A	N/A	N/A	N/A
	MSE (Real-10-sec)	0.1808	0.1338	N/A	N/A	N/A	N/A
2	MSE (Sim-5-sec)	N/A	N/A	N/A	0.2456	0.1162	N/A
	MSE (Real-2-sec)	N/A	N/A	N/A	1.0729	0.1683	N/A
	MSE (Real-10-sec)	N/A	N/A	N/A	0.7895	0.0812	N/A
3	MSE (Sim-5-sec)	0.5229	0.2237	N/A	0.2442	0.1259	N/A
	MSE (Real-2-sec)	1.0657	0.2340	N/A	1.0682	0.1468	N/A
	MSE (Real-10-sec)	0.8864	0.2924	N/A	0.7894	0.1319	N/A
4	MSE (Sim-5-sec)	0.0941	0.9204	0.2800	N/A	N/A	N/A
	MSE (Real-2-sec)	0.1020	0.8102	0.3734	N/A	N/A	N/A
	MSE (Real-10-sec)	0.2694	0.8165	0.4186	N/A	N/A	N/A
5	MSE (Sim-5-sec)	N/A	N/A	N/A	0.2834	0.5460	N/A
	MSE (Real-2-sec)	N/A	N/A	N/A	1.0699	0.6459	0.5795
	MSE (Real-10-sec)	N/A	N/A	N/A	0.9072	0.6453	0.5781
6	MSE (Sim-5-sec)	0.6321	0.9139	0.5245	0.3677	0.8661	0.5331
	MSE (Real-2-sec)	1.0846	0.7509	0.5353	1.0868	0.6039	0.5984
	MSE (Real-10-sec)	0.9875	0.7382	0.5102	0.9447	0.6233	0.5113

Table 4: Summary of Model Performance for each error state for scenarios 1-6 of the sim-5-sec, the real-2-sec, and the real-10-sec datasets.

Discussion

- Network performs well in the absence of ambiguous error sources, reducing the MSE of the active navigation errors.
- Network successfully distinguished between CT shifts caused by CT and D pos errors in real data.
- Increasing aperture length improves performance with blur-related errors.
 - Some degree of learning occurs in most scenarios
- Future work: different aperture lengths, including vehicle/target geometry, more training data.

References

[1] E. C. Zaugg and D. G. Long, "Generalized Frequency Scaling and Backprojection for LFM-CW SAR Processing," *IEEE Trans. Geosci. Remote Sens.*, vol. 53, no. 7, pp. 3600–3614, July 2015.
 [2] C. Lindstrom, R. Christensen, and J. Gunther, "Sensitivity of bpa sar image formation to initial position, velocity, and attitude navigation errors," *arXiv*, vol. abs/2009.10210, 2020.
 [3] S. Zagoruyko, N. Komodakis, "Wide residual networks," *arXiv*, vol. abs/1605.07146, 2016.

Acknowledgments: This research was partially supported by Sandia National Labs on grants 201782, 202136, and 202854. The support and resources from the Center for High Performance Computing at the University of Utah are gratefully acknowledged.